

The COP9 SIGNALOSOME Is Required for Postembryonic Meristem Maintenance in *Arabidopsis thaliana*

Anna Franciosini^{1,5}, Laila Moubayidin^{1,6}, Kaiqi Du^{2,7}, Nahill H. Matari^{2,8},
Alessandra Boccaccini³, Simone Butera¹, Paola Vittorioso³, Sabrina Sabatini³,
Pablo D. Jenik^{2,*}, Paolo Costantino³ and Giovanna Serino^{1,4,*}

¹Dipartimento di Biologia e Biotecnologie “C. Darwin”, Sapienza Università di Roma, Piazzale Aldo Moro 5, 00185 Rome, Italy

²Department of Biology, Franklin & Marshall College, Lancaster, PA 17604-3003, USA

³Istituto Pasteur – Fondazione Cenci Bolognetti, Dipartimento di Biologia e Biotecnologie “C. Darwin”, Sapienza Università di Roma, Piazzale Aldo Moro 5, 00185 Rome, Italy

⁴Institute of Agricultural Biology and Biotechnology, National Research Council of Italy (CNR), via Salaria km 29,300, 00015 Monterotondo Scalo, Rome, Italy

⁵Present address: RIKEN Plant Science Center, Tsurumi, Yokohama, Kanagawa 230-0045, Japan

⁶Present address: Department of Crop Genetics, John Innes Center, Norwich Research Park, Norwich NR4 7UH, UK

⁷Present address: University of Pennsylvania, Masters Program in Biotechnology, Philadelphia, PA 19104, USA

⁸Present address: New York Medical College, Valhalla, NY 10595, USA

*Correspondence: Giovanna Serino (giovanna.serino@uniroma1.it), Pablo D. Jenik (pjenik@fandm.edu)

<http://dx.doi.org/10.1016/j.molp.2015.08.003>

ABSTRACT

Cullin-RING E3 ligases (CRLs) regulate different aspects of plant development and are activated by modification of their cullin subunit with the ubiquitin-like protein NEDD8 (NEural precursor cell expressed Developmentally Down-regulated 8) (neddylation) and deactivated by NEDD8 removal (deneddylation). The CONSTITUTIVELY PHOTOMORPHOGENIC9 (COP9) signalosome (CSN) acts as a molecular switch of CRLs activity by reverting their neddylation status, but its contribution to embryonic and early seedling development remains poorly characterized. Here, we analyzed the phenotypic defects of *csn* mutants and monitored the cullin deneddylation/neddylation ratio during embryonic and early seedling development. We show that while *csn* mutants can complete embryogenesis (albeit at a slower pace than wild-type) and are able to germinate (albeit at a reduced rate), they progressively lose meristem activity upon germination until they become unable to sustain growth. We also show that the majority of cullin proteins are progressively neddyated during the late stages of seed maturation and become deneddyated upon seed germination. This developmentally regulated shift in the cullin neddylation status is absent in *csn* mutants. We conclude that the CSN and its cullin deneddylation activity are required to sustain postembryonic meristem function in *Arabidopsis*.

Keywords: *Arabidopsis thaliana*, cullin-Ring ubiquitin ligase, COP9 signalosome, embryo development, seed maturation, meristem

Franciosini A., Moubayidin L., Du K., Matari N.H., Boccaccini A., Butera S., Vittorioso P., Sabatini S., Jenik P.D., Costantino P., and Serino G. (2015). The COP9 SIGNALOSOME Is Required for Postembryonic Meristem Maintenance in *Arabidopsis thaliana*. *Mol. Plant*. ■ ■, 1–12.

INTRODUCTION

Degradation of selected substrates by the ubiquitin-proteasome system is a major mechanism for the control of plant development. E3 ubiquitin ligases are responsible for adding a chain of ubiquitin molecules to target proteins, promoting their recognition and subsequent degradation by the 26S proteasome. Most plant E3 ubiquitin ligases belong to the Cullin-RING (CRLs)

type (Hotton and Callis, 2008). All CRLs are composed of a backbone cullin subunit (CUL1, CUL3, or CUL4 in *Arabidopsis*) that interacts via its C-terminus with a RING-box protein 1 subunit (RBX1 in *Arabidopsis*), which functions in turn as a platform for the

Molecular Plant

binding of an E2 ubiquitin-conjugating enzyme. At its N-terminus, the cullin subunit binds specific substrate recognition (SR) modules that recognize and deliver the appropriate substrate for ubiquitination (Petroski and Deshaies, 2005). Three main subclasses of CRLs can be found in *Arabidopsis*, based on the type of cullin and the SR: the SCF class (SKP1-CULLIN1-F-BOX), the CRL3 class (containing CUL3), and the CRL4 class (containing CUL4) (Hotton and Callis, 2008).

CRLs are subjected to cycles of activation-deactivation. In a typical CRL activity cycle, substrate binding to the SR triggers the addition of the ubiquitin-like protein NEDD8 (also called RUB1 in plants; Hotton and Callis, 2008) to the cullin subunit (neddylation). Neddylation favors a conformational rearrangement of the cullin C-terminal domain and RBX1, and promotes substrate ubiquitination (Kawakami et al., 2001; Duda et al., 2008). NEDD8 is then removed (deneddylation) by the COP9 signalosome (CSN), an eight-subunit deneddylase (Lyapina et al., 2001; Schwechheimer et al., 2001). The CSN competes with the substrate for CRL binding, and can sterically block substrate access while remaining bound to the CRL, thus keeping it inactive (Schwechheimer et al., 2001; Bennett et al., 2010; Fischer et al., 2011; Enchev et al., 2012; Zemla et al., 2013; Lingaraju et al., 2014). Once de-neddylated by the CSN, the CRL can either change substrate specificity, by binding a different SR module, or interact with a new molecule of the same substrate. Both neddylation and deneddylation are thus necessary to sustain CRL activity, as also demonstrated by genetic analyses (Schwechheimer et al., 2001; Wee et al., 2005; Schmidt et al., 2009; Lydeard et al., 2013).

The essentiality of the CRL deneddylation/neddylation cycle is demonstrated by the severe phenotype caused by its absence. In *Arabidopsis*, lack of any one of the CSN subunit triggers the disaggregation of the complex, and mutants of different CSN subunits show a highly similar phenotype (Wei et al., 2008). Complete loss-of-function mutants of different CSN subunits, where CRL activity is impaired due to lack of deneddylation, arrest growth at the seedling stage (Wei and Deng, 1992; Wei et al., 1994; Schwechheimer et al., 2001; Dohmann et al., 2008a). Analyses of both strong and weak alleles has also shown that CSN controls photomorphogenic development through a CUL4-CDD (COP10, DDB1, and DET1) complex (Chen et al., 2006); hormone signaling through SCF^{TIR1} (auxin), SCF^{COI1} (jasmonic acid) and SCF^{SLY1} (gibberellin [GA]), and CRL4-DDA1 (abscisic acid [ABA]) (Schwechheimer et al., 2001; Feng et al., 2003; Stuttmann et al., 2009; Dohmann et al., 2010; Hind et al., 2011; Irigoyen et al., 2014); flower development through SCF^{UFO} (Wang et al., 2003); and hypocotyl elongation through SCF^{CFK1} (Franciosini et al., 2013). Similar phenotypes, including termination of growth, can be found in seedlings overexpressing point mutants of CSN subunits, which exert a dominant negative defect in cullin deneddylation (Gusmaroli et al., 2004), indicating that a failure in CSN-mediated deneddylation is likely responsible for the majority of developmental defects of *csn* mutants.

The terminal growth defects of *csn* seedlings have been attributed to accumulation of DNA damage and subsequent arrest in the G2 phase of the cell cycle (Dohmann et al., 2008a). However, even though the first *csn* mutants were isolated over 20 years ago (Wei and Deng, 1992), the contributions of CSN

COP9 SIGNALOSOME in *Arabidopsis* Development

function to embryonic and seedling development remain poorly characterized. To address this issue, we performed an in-depth phenotypical analysis of *csn* mutants during embryo development, seed germination, and at early stages of seedling development, and we monitored the cullin deneddylation/neddylation ratio at the same stages. Our data show that, although they develop at a slower rate and have reduced auxin responses, *csn* seeds are able to complete development and to germinate. In contrast, upon germination, *csn* seedlings progressively lose meristem activity until they come to a complete growth arrest. We also show that the majority of cullin becomes progressively neddyated during the last phases of seed maturation, and that this bulk cullin neddylation is reversed upon seed germination. This developmentally regulated shift in the cullin deneddylation/neddylation ratio is absent from *csn* mutants, suggesting that postgerminative meristem function depends on the extensive CRL deneddylation occurring during early germination stages.

RESULTS

csn Mutations Affect the Rate of Seed Germination with and without Stratification

To analyze the effects of the lack of the CSN at early stages of plant development, we used the null *csn2* mutant allele (*fus12-U228*), which bears a loss-of-function mutation in the *CSN2* gene. The *csn2* mutant has no detectable CSN, accumulates neddyated cullins, and shows severe growth defects that eventually lead to growth arrest at the seedling stage (Serino et al., 2003).

We first compared the germination ratio of *csn2* to the hypomorphic *csn5a-2* mutant. *csn5a-2* is deficient in one of the two *CSN5* genes, still accumulates reduced levels of CSN and neddyated cullins, has a semi-dwarf phenotype, and is able to germinate, albeit at a reduced rate (Figure 1) (Serino et al., 2003; Gusmaroli et al., 2004; Dohmann et al., 2005, 2010). Both *csn5a-2* and the *csn2* seeds were able to germinate with or without stratification (Figure 1). As expected, *csn5a-2* germination was delayed compared with the wild-type: without stratification, after 2 days of imbibition (48 hours after imbibition [HAI]), when 80% of Col-0 seeds had germinated, only about 53% of *csn5a-2* seeds were able to germinate (Figure 1A). This percentage rose to 60% if seeds were stratified for 2 days prior to imbibition, as similarly reported by Dohmann et al. (2010) (Figure 1B). *csn2* seeds took even longer to germinate: after 3 days, when 100% of *Ler-0* seeds were germinated, only about 5% of *csn2* seeds were germinated, with (Figure 1A) or without (Figure 1B) stratification; after 8 days (192 HAI), germination of *csn2* seeds reached 19% without stratification (Figure 1A). However, if *csn2* seeds were stratified for 7 days, up to 62% (n = 86) germinated at 2 days after imbibition and up to 100% (n = 31) by 7 days after imbibition (not shown in the figure). Other *csn* null alleles (*csn3*, *csn8*, and *csn5ab*) also germinate well after 7 days of stratification, although the response varies depending on the defective subunit (Dohmann et al., 2010). These results imply that lack of CSN and its deneddylation activity does not prevent seed germination regardless of the stratification. However, the need for extended stratification suggests that CSN-defective mutants are more dormant than their wild-type counterparts, possibly due to the

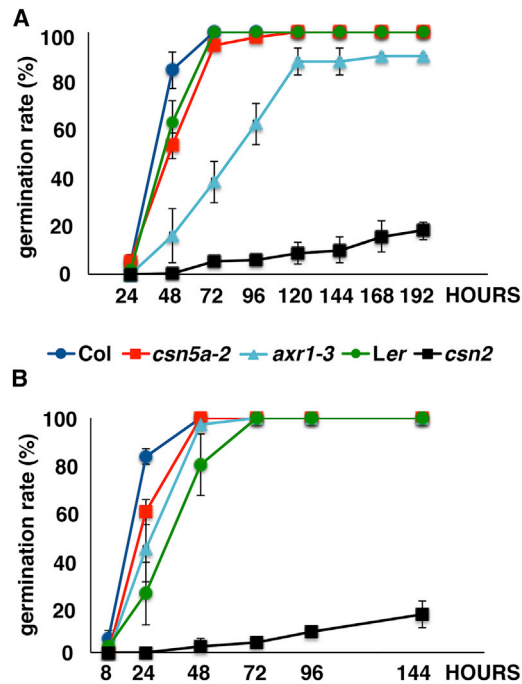


Figure 1. *csn* Mutants Can Complete Germination with or without Stratification.

Germination rates of *axr1-3*, *csn5a-2* (red squares), and *csn2* (black squares) mutants and their respective wild-type ecotype (Col, blue circles) for *axr1-3* and *csn5a* and wild-type siblings (Ler, green circles) for *csn2*. Seeds were grown for the indicated times in white light, without (A) or with (B) stratification. Bars represent the mean \pm SE of three biological repeats ($n \geq 50$ per biological repeat).

reported effects of CSN on GA signaling, which is important in the release from dormancy (Finkelstein et al., 2008; Dohmann et al., 2010). Interestingly, the *axr1-3* mutant, which has reduced neddylation activity (Dharmasiri et al., 2007), behaved similarly to *csn5a-2*, especially when seeds were stratified, indicating that both neddylation and deneddylation promote germination. With no stratification, the germination of *axr1-3* seeds was further delayed and in our experimental conditions did not reach 100% even at 7 days after germination (DAG), suggesting an additional effect of neddylation on the release from dormancy.

***csn* Mutations Affect the Activity of the Root and Shoot Apical Meristem**

We next sought to assess whether the absence of CSN and its deneddylation activity had early effects on seedling development, after germination and prior to growth arrest. Because the root is the first organ that develops postembryonically and because growth-arrested *csn2* mutants, similarly to other *csn* mutants, display a short root (Supplemental Figure 1) (Kwok et al., 1996), we monitored root meristem growth in *csn2* (Figure 2). We measured the size of the *csn2* root apical meristem (RAM) over time by counting the number of cortex cells in a file extending from the quiescent center (QC) to the first elongated cell (Dello Iorio et al., 2007). To discriminate the effects of the lack of CSN related to its activity from those due to downstream defects in the light-related pathways in which CSN is involved, we carried out the same analysis on the RAM

of the *cop1-5* mutant, which has the same light-related defects as the *csn* mutants (constitutive photomorphogenesis) but has normal CSN levels, a normal cullin neddylation pattern, and a milder root meristem defect (Kwok et al., 1998; Schwechheimer et al., 2001; Sassi et al., 2012).

The time-course analysis of the RAM showed that the size of *csn2* root meristems, but not of *cop1-5* meristems, rapidly decreased over time compared with the wild-type, and virtually disappeared at 6 DAG (Figure 2A). Indeed, cells of the *csn2* root meristem were almost completely differentiated already at 5 DAG (Figure 2B and 2C), while *cop1-5* roots still had a functional RAM, albeit reduced in size (Figure 2D and 2E). Decreased meristem size could be due to reduced cell-division activity of the meristematic cells; indeed, it has been shown that terminally growth-arrested *csn* mutants have defects in cell-cycle progression (Dohmann et al., 2008a). We therefore determined the cell-division activity of *csn2* root meristems at 3 DAG by visualizing cells in the G2/M phase using the *pCYCLINB1;2-GUS* (*pCYCB1;2-GUS*) reporter (Donnelly et al., 1999; Adachi et al., 2006; Dekkers et al., 2013). *pCYCB1;2-GUS* is a true reporter for G2/M, as opposed to *pCYCB1;1-GUS*, which is induced by DNA damage (Culligan et al., 2006). As shown in Figure 2F–2I, the fraction of GUS-stained cells over total number of cells (hence the cell-division rate) was the same in *csn2* roots as in the wild-type, suggesting that the observed shortening and subsequent disappearance of the root meristem in the mutant was not primarily due to a cell-cycle arrest in the G2/M phase.

We thus asked whether the QC activity, responsible for maintaining the stem cell initials, was altered in *csn2* mutants. To this end, we monitored the expression of the QC-specific markers QC46 (Figure 2J and 2M) and QC25 (Figure 2N and 2Q) (Sabatini et al., 1999). The expression of both markers was reduced in *csn2* meristems at three DAG (Figure 2K and 2O), suggesting a reduction in QC activity. As a consequence of reduced QC activity, cells immediately below the QC at the position of columella stem cells acquired differentiation markers such as amyloplasts and Q1630 (Sabatini et al., 2003) (Figure 2K, 2R, and 2S). A similar phenotype was also observed in *csn4* root meristems (Supplemental Figure 2A). Almost no QC reporter expression could be detected in *csn2* terminally growth-arrested roots (7 DAG; Supplemental Figure 2B), suggesting that the growth arrest observed in *csn* roots was due to a progressive loss of QC identity. On the contrary, QC identity was not affected in *cop1-5* mutant, as QC46 and QC25 expression was correctly retained (Figure 2L, 2M, 2P, and 2Q), and no amyloplasts were found in columella stem cells (Figure 2M), in agreement with the relatively healthy RAM of *cop1-5* seedlings.

Auxin is necessary for QC specification (Sabatini et al., 1999), and the CSN regulates auxin signaling by interacting directly with SCF^{TIR1} (Schwechheimer et al., 2001). Growth-arrested (at 7 DAG) *csn3*, *csn4* and *csn5* mutants have impaired auxin responses and a reduced activity of the auxin reporter *DR5:GUS* (Schwechheimer et al., 2001; Dohmann et al., 2008b). We noticed that *DR5:GUS* expression was already reduced in *csn2* root meristems at 3 DAG (Figure 2T and 2U), suggesting that a reduction in auxin response could be responsible for the progressive loss of QC identity in CSN-defective mutants.

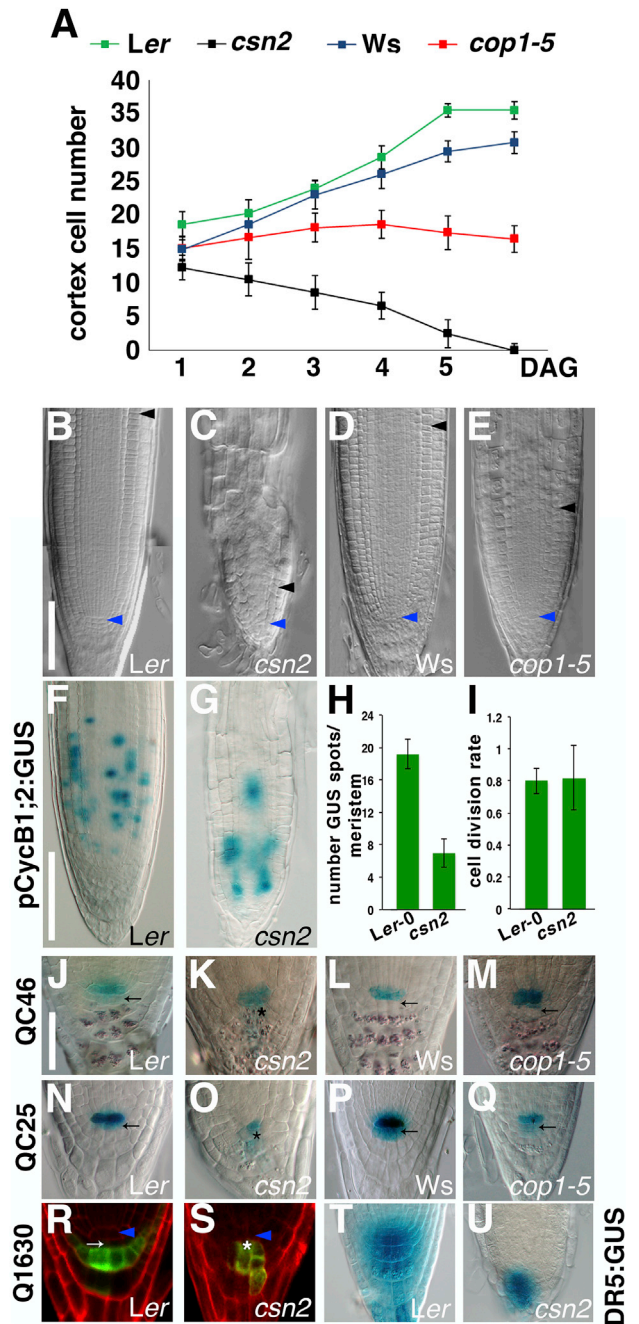


Figure 2. *csn* Mutants Fail to Sustain Root Meristem Activity.

(A) Cortex cell number of segregating wild-type siblings (*Ler* and *Ws*, green and red squares, respectively), *csn2* (black squares) and *cop1-5* (red squares) root meristems at 2–6 days after germination (DAG).

(B–E) Photographs of root meristems of *csn2* (C), *cop1-5* (E), and their relative wild-type siblings (B and D, respectively) at 5 DAG. Blue arrowheads indicate the first cortex cell; black arrowheads indicate the last cortex cell.

(F and G) *pCYCB1;2:GUS* expression in 3 DAG segregating wild-type siblings and *csn2* root meristems.

(H and I) *pCYCB1;2:GUS*-stained spots per meristem (H) and cell-division rate (number of GUS-stained cells per meristem) (I) of wild-type segregating siblings and *csn2* at 3 DAG, roots, $n = 50$.

(J–U) *QC46* (J–M), *QC25* (N–Q), *Q1630* (R–S), and *DR5:GUS* (T–U) expression and amyloplasts (lugol) staining in 3 DAG wild-type segregating siblings (J, N, R, T from *CSN2/csn2* plants; L, P from *COP1/cop1-*

csn2 seedlings also showed defects in shoot apical meristem (SAM) function (Figure 3). The first two true leaf primordia in wild-type seedlings start growing at 2 DAG (Figure 3A), and by 7 DAG several leaves have formed (Figure 3B). In contrast, the first true leaf primordia in *csn2* seedlings do not appear until 5 DAG and never grow afterward (Figure 3C and 3D; Kwok et al., 1996); no further leaf primordia ever forms in the mutants. This suggests that the SAM is functional after germination but loses its ability to produce new organs shortly after. This phenotype is correlated with the expression level of *pSHOOTMERISTEMLESS:GUS* (*pSTM:GUS*), which is expressed in the SAM throughout embryogenesis (Figure 3A and 3B) (Jurkuta et al., 2009) and is required for meristem activity (Barton and Poethig, 1993). In *csn2* seedlings, *STM* expression, although correctly localized, is already reduced compared with the wild-type at 2 DAG and it remains significantly lower until growth arrest at 7 DAG (Figure 3C and 3D).

csn Mutations Cause Mild Embryonic Defects, Primarily in the Root Stem Cell Niche

To determine whether the root stem cell niche defects and the (smaller) alterations in the activity of the SAM start after germination or originate during embryonic development, we characterized embryogenesis in the *csn2* mutant in detail.

The first defect we noticed was that there were only $15.6 \pm 2\%$ mutant seeds (four independent experiments), instead of the expected 25% in the siliques of heterozygous *CSN2/csn2* plants. Reciprocal crosses between *CSN2/csn2* and wild-type sibling plants clearly indicated that transmission was reduced through the male. The expected 1:1 ratio of wild-type and heterozygous plants in the F1 generation was obtained when wild-type plants were used as pollen donors ($\chi^2 = 0.026$, $p = 0.87$; $n = 148$). However, when *CSN2/csn2* plants were the pollen donors, we observed only 32% heterozygotes in the F1 generation, a very significant deviation from the expected 50% ($\chi^2 = 21.12$, $p < 0.0001$; $n = 138$).

After fertilization, development of *csn2* embryos and endosperm proceeded at a slower rate than that of wild-type embryos in the same silique (Figure 4, Supplemental Table 1, and Supplemental Figure 3A and 3B), indicating that lack of CSN affects the rate of cell division during embryogenesis. However, similar to seedlings, the percentage of cells expressing the *pCYCB1;2:GUS* reporter was similar for wild-type and *csn2* embryos at the heart ($1.1 \pm 0.6\%$ [$n = 16$] vs $0.9 \pm 0.3\%$ [$n = 6$]) or late heart ($0.8 \pm 0.7\%$ [$n = 17$] vs $0.8 \pm 0.7\%$ [$n = 8$]) stages, suggesting that the developmental delay was not due to defects in the G2/M phase. Despite the cell-cycle delay, mutant embryos appeared normal until the 16-cell stage, when we observed abnormal cell-division planes, particularly in the hypophysis and its derivatives. At this stage, it is not yet possible to separate wild-type and mutant embryos (Supplemental Table 1) but wild-type embryos never show these defects (Jenik et al., 2005). After the early globular stage, when *csn2* embryos are clearly

5 plants), *csn2* (K, O, S, and U), and *cop1-5* (M, Q) seedlings. Black and white arrows indicate the columella stem cells. Blue arrowheads indicate the QC. Black and white asterisks indicate the presumptive position of columella stem cells in the *csn2* mutant. Scale bar represents 100 μm for (B–E), 50 μm for (F–G), 50 μm for (J–U).

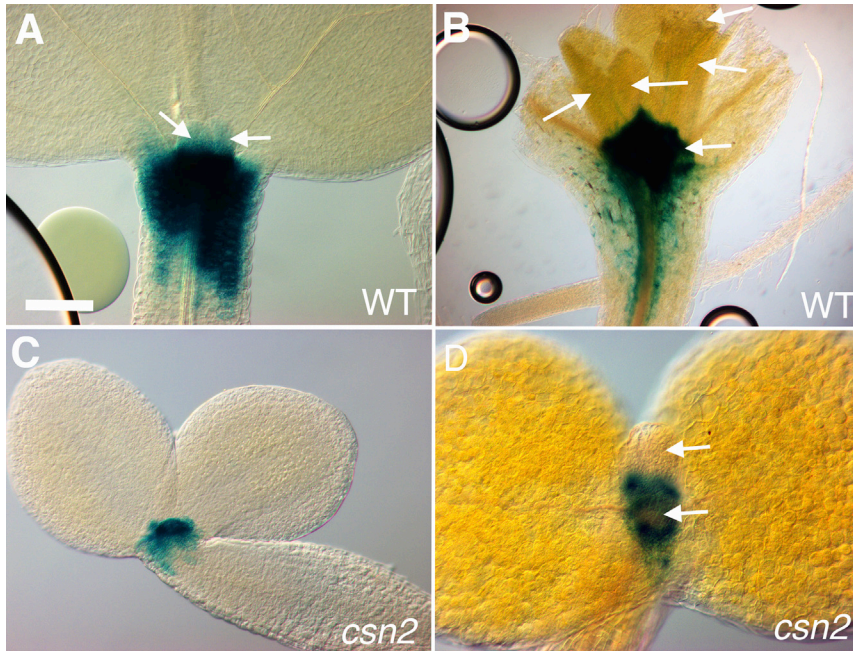


Figure 3. *csn* Mutants Have Defects in the Shoot Apical Meristem.

pSTM:GUS expression in segregating wild-type siblings (A and B) and *csn2* seedlings (C and D) at 2 DAG (A–C), and 7 DAG (B–D). The arrows point to the true leaf primordia (A and D) or true leaves (B). Scale bar represents 80 μm for (A, C, and D); 160 μm for (B).

distinguishable because they are delayed, 57% of mutant embryos show defects ($n = 68$) compared with just 4% of wild-type embryos ($n = 52$) (Figure 4A and 4B). These early defects resulted in a disorganized root pole by the late heart stage, concomitant with the accumulation of anthocyanin pigments in the apical portion (Figure 4C and 4D and Supplemental Figure 3C–3E).

These results prompted us to determine whether the QC was properly established in the embryo by analyzing the expression of four different reporter genes: *QC25*, *QC46*, *pWUSCHEL-RELATED HOMEBOX5:GFP* (*pWOX5:GFP*) (Blilou et al., 2005), and *pSCARECROW:GFP* (*pCSR:GFP*) (Wysocka-Diller et al., 2000) (Figure 4E–4L). *QC25* and *QC46* expression could be observed, albeit at slightly reduced levels, in 57.3% ($n = 68$) and 66% ($n = 47$) of *csn2* embryos, respectively (Figure 4E–4H). The QC marker *pWOX5:GFP* expression was absent in only 12% ($n = 50$) of mutant embryos (Figure 4I and 4J). Furthermore, expression of the root endodermis and QC marker *pCSR:GFP* was also similar in *csn* mutants and in their wild-type siblings (Figure 4K and 4L). These results indicate that the CSN is not strictly necessary for the establishment of the stem cell niche during embryogenesis.

The hypophysis and QC defects observed at the embryo root pole are reminiscent of defects in auxin production, transport, or response (Möller and Weijers, 2009). To evaluate these processes in CSN-defective embryos, we analyzed the expression of a reporter gene that reflects auxin transport (*pPIN1:PIN1-GFP*, a translational fusion of PIN-FORMED1 [an auxin efflux carrier], and GFP; Gordon et al., 2007), and of a reporter for auxin response (*DR5rev:GFP*; Friml et al., 2003). While auxin transport did not seem to be affected ($n = 23$; Figure 4M and 4N), auxin response was consistently reduced in *csn2* embryos ($n = 62$; Figure 4O and 4P). The embryo defects observed in *csn2* embryos were also observed in the null *csn4* mutant (*cop8-1* allele), but not in *cop1-5* embryos (data not shown and McNellis et al., 1994). This suggests that

an impairment in auxin perception could be one of the causes of the subsequent loss in QC activity of *csn2* seedlings, implying that lack of CSN in its deneddylation activity is necessary postembryonically to sustain stem cell activity in the root meristem.

Similar to the SAM, reduced *STM* expression was already detectable in *csn2* embryos (Figure 4Q and 4R). In contrast, the enhancer trap *M0233*, which reflects the expression of *CUP-SHAPED COTYLEDONS1* at the boundary between the meristem and the cotyledons (Cary

et al., 2002), was properly localized and expressed at normal levels in *csn2* embryos (Figure 4S and 4H). These results suggest that *csn* mutants can form an SAM in the embryo, although it is unclear whether it is fully functional. CSN-defective mutants are likely unable to maintain an active population of shoot meristematic cells postembryonically.

CUL1 Neddylation Increases During Seed Maturation and Decreases During Seed Germination

We next sought to monitor the cullin deneddylation/neddylation ratio at the same developmental stages analyzed in the previous sections. We first assessed the neddylation profile of the SCF subunit CUL1, a known CSN substrate (Lyapina et al., 2001; Schwechheimer et al., 2001), during late seed development and seed maturation starting at 8 days after pollination (DAP) (Figure 5). At 8 and until 13 DAP, the CUL1 neddylation level resembled that observed for CUL1 in seedlings, with the majority of SCF in its deneddylated form (Schwechheimer et al., 2001). However, at 16 DAP, concomitant with embryo dehydration, CUL1 progressively accumulates in its neddylated form, with CUL1 neddylation reaching its highest level in mature dry seeds (Figure 5A, top). By densitometric analysis, we estimated that while 38% of total CUL1 was neddylated in embryos at 8 DAP, this percentage rose to 65% in dry seeds (Figure 5A, bottom). Since CSN is the major CRL deneddylation, we then assessed whether the reduced CRL deneddylation in dry seeds could be due to a reduced level or partial inactivity of the CSN at that stage. An initial query of the publicly available transcriptome database at the Arabidopsis eFP browser revealed that all CSN subunit transcripts are expressed throughout embryogenesis and seed maturation, albeit with some differences between subunits (<http://bar.utoronto.ca/efp/cgi-bin/efpWeb.cgi>; (Winter et al., 2007; Le et al., 2010)). To confirm these data, we assessed the abundance of selected CSN subunits (CSN2, -4, -5, and -6) in dry seeds through immunoblot analysis. We found that all the

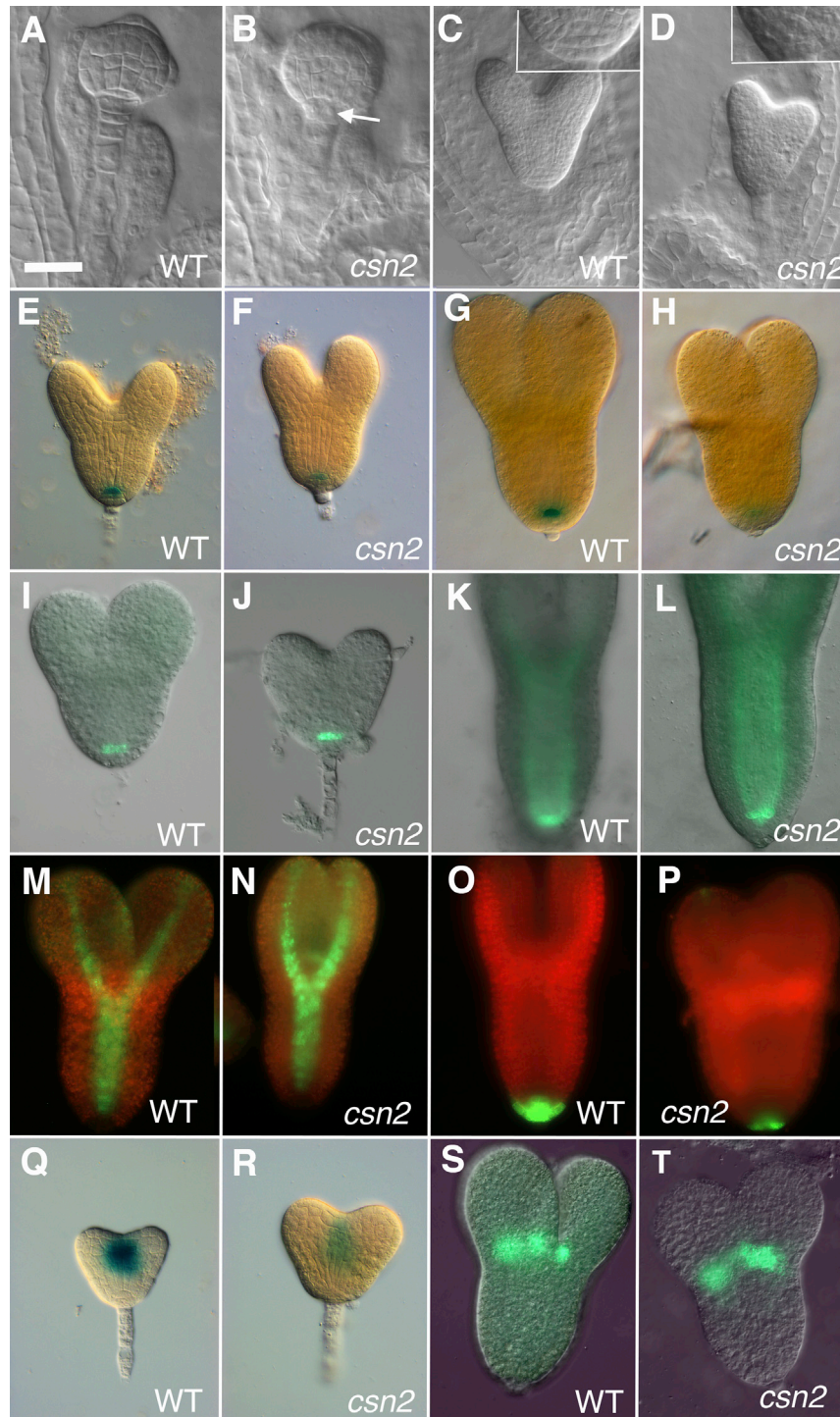


Figure 4. The Root and Shoot Meristems Are Properly Established in a Majority of *csn* Embryos.

(A–D) Embryo phenotypes of mid-globular stage (A and B) and late heart stage (C and D) wild-type siblings (A and C) or *csn2* (B and D) embryos. The arrow in (B) points to abnormal division of the hypophysis in *csn2*. The insets show the root pole (abnormally patterned in *csn2*) at higher magnification. Wild-type and *csn2* embryos have been paired so that they are the same stage, not age (i.e., *csn2* embryos are from older siliques than their wild-type *Ler* counterparts).

(E–T) Expression of *QC25* (E and F), *QC46* (G and H), *pWOX5:GFP* (I and J), *pSCR:GFP* (K and L), *pPIN1:PIN1-GFP* (M and N), *DR5rev:GFP* (O and P), *pSTM:GUS* (Q and R), and *M0233* (S and T) in wild-type (E, G, I, K, M, O, Q, and S) or *csn2* (F, H, J, L, N, P, R, and T) embryos. Stages: heart (E–F, I–J, and Q–R), late heart/early torpedo (G–H), mid-torpedo (K–P, S–T). Embryos have been paired according to stage, not age. For each pair, embryos were stained (GUS) or exposed (GFP) for the same length of time. Scale bar represents 10 μ m for (A and B) and insets in (C and D); 20 μ m for all other panels.

we assayed for cullin neddylation in developing seeds of the *csn5a-2* hypomorph. *csn5a* mutants are viable and fertile, thus allowing us to analyze them at this developmental stage (Serino et al., 2003; Gusmaroli et al., 2004; Dohmann et al., 2005). As shown in Figure 5B, and consistent with previous observations made on *csn5a-2* seedlings (Gusmaroli et al., 2004; Dohmann et al., 2005), CUL1 accumulated mostly in its neddylation form in *csn5a-2* developing seeds. This confirms the central role of the CSN in CUL1 deneddylation/neddylation dynamics at this stage of plant development.

To assess whether the increase in CUL1 neddylation observed in mature dry seeds (Figure 5A) is reversed during seed germination, we compared the CUL1 neddylation profile in dry and germinating seeds (Figure 6). We found that the majority of CUL1 was deneddylation 24 HAI of the seeds (Figure 6A, top). By densitometric analysis, we estimated that

subunits analyzed were present at similar levels in both dry seeds and seedlings (Supplemental Figure 4). Because CSN subunits (except for CSN5) accumulate to proper levels only when the whole complex is present (Wei et al., 2008), these data indicate that the CSN holocomplex is present in dry seeds and suggest that it is partially inactive rather than present in lower amount.

To further confirm that the shift in the CUL1 deneddylation/neddylation ratio during seed maturation is controlled by the CSN,

the fraction of neddylation CUL1 dropped from 65% in dry seeds to about 35% in 24 and 48 HAI seedlings (Figure 6A, bottom). This drop in CUL1 neddylation seems to take place rather early in seed germination, since the percentage of neddylation CUL1 appeared to decrease constantly over time starting as early as at 4 HAI (Figure 6B). In contrast, NEDD8-CUL1 conjugates accumulated constitutively in *csn5a-2* germinating seeds, confirming that the CSN mediates this process (Figure 6C).

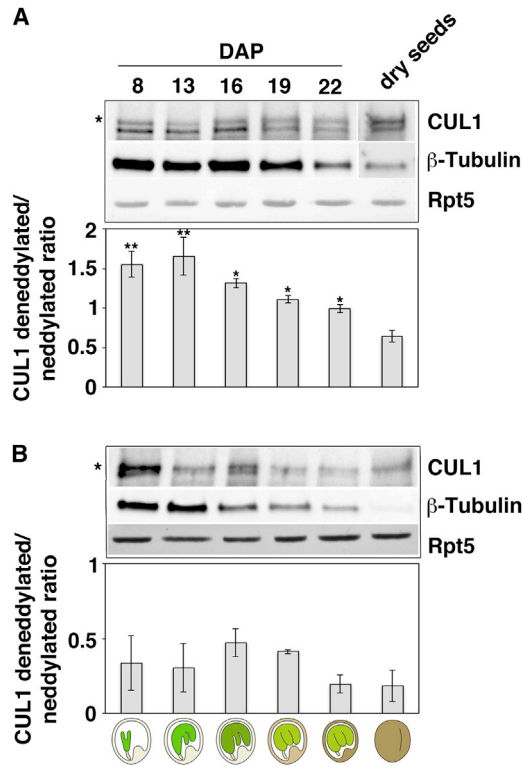


Figure 5. The CUL1 Neddylation Status Changes During Seed Maturation and Is Dependent on the CSN.

Total protein extracts from embryos at 8, 13, 16, 19, and 22 days after pollination (DAP) and from mature dry seeds from Col wild-type (WT) (A) or *csn5a-2* (B) were subjected to immunoblot analysis with antibodies to CUL1 (top panel). Rpt5 was used a loading control. β -Tubulin was used to indicate development arrest in embryos (Raz et al., 2001). Asterisks at the left of the immunoblots indicate NEDD8-CUL1 conjugates. The lower panels show quantification as a mean of the ratio between deneddylated to neddylated CUL1 \pm SE (n = 3), and asterisks in the graphs indicate $p < 0.05$ (*) or $p < 0.01$ (**) relative to dry seed values.

These results indicate that a major peak of CUL1 neddylation occurs at the dry seed stage, which is reversed during seed imbibition. Interestingly, a survey of the transcriptomic data publicly available at the eFP browser indicated that the transcript levels of CSN subunits tend to remain stable or to increase in the first hours of seed germination, probably sustaining the deneddylation process (Winter et al., 2007; Dekkers et al., 2013).

Seed Neddylation Dynamics Are a Common Feature of CUL1, CUL3, and CUL4

We next asked whether the changes in the CUL1 neddylation profile during seed maturation and germination are specific to CUL1, or whether they are shared by other *Arabidopsis* cullins, such as CUL3 and CUL4 (Figure 7). Both CUL3 and CUL4 have been shown to be mainly present in their deneddylated form in seedlings and their neddylation status is controlled by the CSN (Dieterle et al., 2005; Figueroa et al., 2005; Chen et al., 2006). We found that all three cullins share a similar neddylation profile at 8 DAP, becoming more neddylated in dry seeds and reverting to a mostly deneddylated form upon seed imbibition (Figure 7A). More specifically, about 63% and 62% of total CUL3 and CUL4, respectively, was neddylated in dry seeds,

whereas at 48 HAI this fraction dropped to only 34% and 38% (Figure 7A). This result was also corroborated by immunoblot analysis with an anti-NEDD8 antibody, which confirmed accumulation of NEDD8-Cullin conjugates as well as of free NEDD8, in dry seeds (Figure 7B). This increase in free NEDD8 in dry seeds might be, in addition to a possible CSN deactivation mentioned above, one of the causes of the increase in cullin neddylation observed at this developmental stage; it also further indicates that NEDD8 levels are developmentally regulated. Another major developmental switch for *Arabidopsis*, the light versus dark seedling growth did not bring about any major remodeling of the cullin neddylation profile (Supplemental Figure 5), suggesting that this may be mostly related to the transition from dry to imbibed seeds.

DISCUSSION

CSN Function Is Necessary for Meristem Maintenance

CSN-defective mutants, in which CRLs are constitutively neddylated, can still complete embryogenesis and seed germination (this study; Dohmann et al., 2010). Our reporter gene analysis shows that, other than in the root pole, the patterning of *csn2* embryos appears normal, and that genes normally present in the SAM and RAM are expressed, albeit at reduced levels (Figure 4). Thus, CSN-mediated CRL deneddylation is not essential for embryo development. Upon germination, however, activity in the root and shoot meristems of *csn* mutants decreases progressively: the expression of QC and SAM markers progressively diminishes during the first 5 DAG (Figures 2J–2Q and 3), and almost no reporter expression can be detected in terminally arrested roots (Supplemental Figure 2), indicating that *csn* mutants are unable to maintain an active population of meristematic cells both at the root and at the shoot apex. As a result, cells differentiate terminally at both apices, indicating a failure in maintaining an active stem cell niche, and leading to growth arrest in these mutants. Interestingly, a recent report points to a similar role of the CSN in maintaining self-renewal of the *Drosophila* germline stem cells (Pan et al., 2014; Qian et al., 2015), suggesting that this function of the CSN might be conserved across phyla. However, the underlying molecular mechanism might be different, given that plant and animal stem cells, although sharing similar structural features, are governed by unique molecular pathways (for a review, see Heidstra and Sabatini, 2014).

Our results also suggest that, in maintaining the activity of the root meristem, the CSN works in a pathway that is light-independent but related to auxin (Figures 2 and 4). Indeed, consistent with previous reports (Schwechheimer et al., 2001; Dohmann et al., 2008b), our results demonstrate that auxin response is reduced in *csn* embryos and seedlings, which may prime the subsequent failure of *csn* mutants to maintain a healthy stem cell population. The CSN is known to regulate the activity of SCF^{TIR1} (Schwechheimer et al., 2001; Dohmann et al., 2008b) and possibly of all the auxin-regulatory CRLs (SCF^{TIR1/AFB}) (Dharmasiri et al., 2005). Furthermore, auxin has emerged not only as the central regulator of stem cell activity and organogenesis at the RAM but also at the SAM (reviewed by Heidstra and Sabatini, 2014). In common with many auxin pathway-related mutants that affect the meristems (reviewed

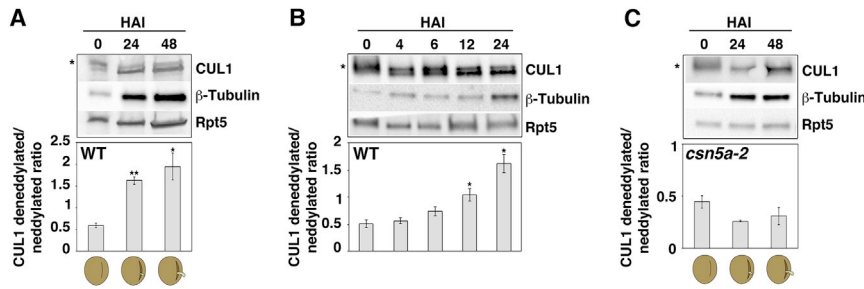


Figure 6. The CUL1 Neddylation Status Changes During Seed Germination.

(A) Mature dry seeds show markedly increased CUL1 neddylation compared with germinating seeds. Total protein extracts from dry (0) or imbibed seeds for the indicated time points were subjected to immunoblot analysis with antibodies to CUL1.

(B) CUL1 neddylation levels decrease upon seed germination. Total protein extracts from dry (0) or imbibed seeds for the indicated time points were subjected to immunoblot analysis with antibodies to CUL1.

(C) The CUL1 deneddylation/neddylation ratio does not change in *csn* seeds. Total protein extracts from dry (0) or imbibed *csn5a-2* seeds for the indicated time points were subjected to immunoblot analysis with antibodies to CUL1.

Rpt5 was used as a loading control. β -Tubulin was used to indicate development arrest in embryos. Asterisks at the left of the immunoblots indicate NEDD8-CUL1 conjugates. The lower panels show quantification as a mean of the ratio between deneddylated to neddylated CUL1 \pm SE (n = 3), and asterisks in the graphs indicate $p < 0.05$ (*) or $p < 0.01$ (**) relative to dry seed values. HAI, hours after imbibition; WT, wild-type (Col).

by M \ddot{o} ller and Weijers, 2009), the *csn* mutants are able to complete embryogenesis and germinate, with growth arrest occurring only after germination. It is possible to imagine that, in the absence of the CSN, a certain degree of activity of SCF^{TIR1/AFB} and other CRLs may still be in place during embryo development and germination. CSN function and CRL deneddylation, however, could become essential for postgerminative development, when most likely a major reprogramming of CRL specificity must take place in order to redirect the cells toward new developmental pathways. It could therefore be speculated that the SR exchange could not occur anymore in the *csn* seedlings, thus not allowing the CRLs, including SCF^{TIR1/AFB}, to acquire new substrate specificity, eventually leading to a complete cell-cycle and growth arrest.

Dohmann et al. (2008b) have argued that the growth defects observed in *csn* seedlings are due to extreme delay or arrest in the G2 phase of the cell cycle, possibly as a consequence of the accumulation of DNA damage. However, their analyses were conducted at 7 DAG, when seedlings had already stopped growing. At earlier stages, we do not detect a delay in G2/M but rather a progressive differentiation of stem cell tissues (Figure 2). Possibly, the accumulation of DNA damage and the induction of DNA repair pathways might be a consequence and not a cause of the dysfunctional meristems. Alternatively, it can be speculated that the higher damage levels, together with the reduced auxin response observed in the *csn* mutants, could directly affect QC cells function and their capability to generate new stem cells, thus causing stem cell differentiation. Further research on these pathways during the first few days after germination of *csn* seedlings will be necessary to sort out these competing hypotheses.

The Ratio of Cullin Deneddylation/Neddylation Is Developmentally Regulated in *Arabidopsis*

Our results show that the cullin deneddylation/neddylation ratio is developmentally regulated in *Arabidopsis*; we show that cullins become progressively neddylated in the late phases of seed maturation, remain neddylated in dry seeds, and undergo a major deneddylation during the first hours of seed imbibition. This shift in the cullin deneddylation/neddylation ratio does not occur in *csn* mutants, in which cullins are constitutively neddylated (Figures 5 and 6; Supplemental Figure 6). We also noticed that the balance

of deneddylated versus neddylated cullin seems to be constant during vegetative growth, since, under our experimental conditions, both embryos and seedlings have the same relative amount (about 65%) of deneddylated versus neddylated cullin, indicating that the cullin deneddylation/neddylation ratio is tightly regulated during plant growth. It is also worthwhile noting that *csn5a-plantlets*, which have very low but detectable levels of deneddylated cullins, are still able to develop into fairly normal adult plants, while *csn2* severe mutants, in which deneddylated cullins are completely absent, show growth arrest at the seedling stage. This suggests that even a residual deneddylation activity (such as that present in *csn5a-2* mutants) is sufficient to allow the transition to the adult phase.

Two reports have recently described a similar modification in the cullin deneddylation/neddylation ratio in widely different biological systems, suggesting that drastic changes in this ratio may be associated with developmental, physiological, or metabolic changes in the cells. A dramatic difference in the neddylation status of Cdc53/Cul1 has been observed when yeast cells are shifted from fermentable to non-fermentable carbon sources and vice versa (Zemla et al., 2013). In addition, activation of tyrosine kinase signaling leads to deneddylation of multiple cullins in T- and B-cells, as well as in a number of other mammalian cell types, from mouse embryonic fibroblasts to human cancer cell lines (Friend et al., 2013). In all these cases, including ours, CSN activity is essential to mediate the shift in the cullin deneddylation/neddylation ratio.

Our results do not allow us to establish whether neddylated cullins in mature dry seeds are part of a CRL complex; if this is the case, however, it is possible that, similar to yeast (Zemla et al., 2013), these neddylated CRLs are already loaded with the substrates, stored in the dry seed, and ready to be active once metabolism and development resume upon imbibition. Our results suggest that the upregulation in cullin neddylation could be due to at least two factors: the overall increase in both free and conjugated Nedd8 levels that we observed in dry seeds (Figure 7B); and, given that the CSN holocomplex is present in dry seeds (Supplemental Figure 4A), a reduced deneddylation activity of the CSN. The CSN might be partially or fully deactivated during the last phases of seed maturation, becoming activated again upon water imbibition. For example, the CSN could be kept dissociated from the CRL in dry seeds

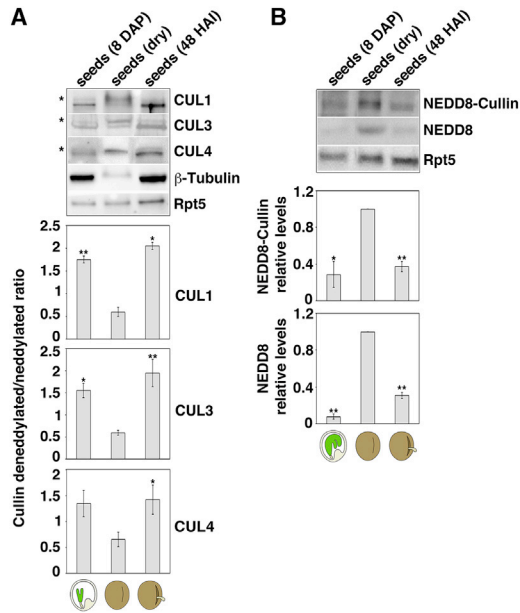


Figure 7. The CUL3 and CUL4 Neddylation Status During Late Embryogenesis, Seed Maturation and Germination Overlaps with CUL1.

(A) CUL1, -3, and -4 neddylation status in embryos (8 DAP), mature dry seeds, and seeds at 48 hours after imbibition (HAI). Total protein extracts were subjected to immunoblot analysis with antibodies to CUL1, -3, and -4 (top panel). Asterisks at the left of the immunoblots indicate NEDD8-Cullin conjugates. The lower panels show quantification as a mean of the ratio between deneddylated to neddylated CUL1, -3, or -4 \pm SE ($n = 3$). (B) Cullin neddylation was confirmed with antibodies to NEDD8 (top panel). Lower panels show quantification as a mean of NEDD8-Cullin conjugates or of free NEDD8 \pm SE ($n = 3$), with the value in dry seeds set to 1. Asterisks in the graphs indicate $p < 0.05$ (*) or $p < 0.01$ (**) relative to dry seed values. Rpt5 was used a loading control. β -Tubulin was used to indicate development arrest in embryos.

by specific factors; recently, UV-elicited dissociation between CSN and CRL4 has been shown to be mediated by the small molecule IP7, suggesting that such factors could indeed exist (Rao et al., 2014). Given that at least two CSN-interacting CRLs (SCF^{COI1} and SCF^{TIR1/AFB1}) are known to bind IP5 and IP6, a similar scenario could be also envisaged for *Arabidopsis* (Rao et al., 2014; Shabek and Zheng, 2014). In addition, plant hormones could also be involved in the regulation both of Nedd8 levels and of the cullin deneddylation/neddylation ratio. For example, ABA is essential to repress both seed dehydration and germination, showing a peak of accumulation toward the end of seed development overlapping the accumulation of the NEDD8-cullin conjugates, and could thus represent a likely candidate. Future experiments should shed light on these hypotheses.

METHODS

Plant Material and Growth Conditions

The *csn2* (*fus12-U228*), *csn4* (*cop8-1*), *cop1-5*, and *csn5a-2* mutants are in the *Arabidopsis thaliana* Landsberg erecta (*Ler*), Wassilewskija (*Ws*) (*csn4* and *cop1-5*), and Columbia (*Col*) accessions, respectively (McNellis et al., 1994; Misera et al., 1994; Wei et al., 1994; Gusmaroli et al., 2004; Dohmann et al., 2005). *pSTM::GUS*, *M0233*, *pSCR::GFP*, *QC25*, *QC46*,

pWOX5::GFP, *DR5rev::GFP*, *pPIN1::PIN1-GFP*, have been described previously (Sabatini et al., 1999; Wysocka-Diller et al., 2000; Cary et al., 2002; Friml et al., 2003; Blilou et al., 2005; Gordon et al., 2007; Jurkuta et al., 2009) and were crossed into the *CSN2/csn2* heterozygous mutant. *Q1630* is from the Haseloff collection (<http://arabidopsis.info/CollectionInfo?id=24>). Unless otherwise noted, *Arabidopsis* seedlings were surface-sterilized and grown on solid Murashige and Skoog medium with Gamborg's vitamins (Duchefa) and 1% sucrose at 22°C with a light intensity of 130 $\mu\text{mol} \cdot \text{m}^{-2} \cdot \text{s}^{-1}$. For crosses and the analysis of embryos, plants were grown in MetroMix 360 soil (SunGro Horticulture) in a greenhouse at 22–24°C with continuous light.

Seed Germination Assays

All seeds used for germination tests were harvested from mature plants grown at the same time, in the same conditions, and/or stored for the same time under the same conditions, except when freshly harvested seeds were used. Mature dry seeds were stored for at least 1 month (30 days) prior to the experiments. Germination assays were performed according to Gabriele et al. (2010). Stratification was conducted by storing seeds for 2 days at 4°C unless otherwise indicated in the text. At least 50 seeds were measured per time point. All germination assays were repeated with three seed batches, and one representative experiment is shown. Student's *t*-test was used for data validation (<http://graphpad.com/quickcalcs/ttest2.cfm>).

Histochemistry and Microscopy

The dissection, clearing, and staining of seeds and seedlings for morphological and reporter analysis were performed as described previously (Dello Iorio et al., 2007; Willmann et al., 2011). Confocal images of median longitudinal sections of roots were taken using a Zeiss LSM 780 microscope. A 10 $\mu\text{g}/\text{ml}$ propidium iodide (Sigma) solution was used to visualize the cell wall. For GUS staining, seedlings were imaged using the Axio Imager.A2 (Zeiss) microscope. For embryos, microscopy was done on a Leica DMRB microscope (Leica Microsystems). Images were acquired with either a ProgRes MFcool or a ProgRes C5 camera (Jenoptik). Images taken on different channels were merged with the ProgRes software. Image contrast, brightness adjustment, and assembly of figures was done with Adobe Photoshop CS5 and CS6 (Adobe Systems).

Root Length and Meristem Size Analysis

Seedlings were grown on vertical plates for the days indicated in the text. Root meristem size was expressed as the number of cortex cells in a file extending from the QC to the first elongated cortex cell, excluded, as described previously (Dello Iorio et al., 2007). For each experiment, a minimum of 30 plants were analyzed. Student's *t*-test was used for data validation (<http://graphpad.com/quickcalcs/ttest2.cfm>). For cell-division rate measurements, β -glucuronidase activity was visualized after 1 h of staining. The cell-division rate index is equal to GUS-stained cells/meristem cell number \pm SEM (Dello Iorio et al., 2007). For each experiment, a minimum of 30 plants were analyzed.

Protein Extraction and Immunoblot Analyses

For protein extraction from *Arabidopsis*, plant material was frozen using liquid nitrogen and then homogenized in denaturing buffer (100 mM Na₂HPO₄, 10 mM Tris-HCl, 8 M urea, pH 8.0). The debris was removed by centrifugation at 20 000 *g* for 10 min at 4°C. Protein samples were boiled for 10 min and then centrifuged 15 000 *g* for 10 min at 4°C (Franciosini et al., 2013). CUL1, CUL3, CUL4, CSN2, CSN5, CSN6, NEDD8, and Rpt5 (Regulatory Particle 5a or At6A) were detected with specific antibodies (Gray et al., 1999; Kwok et al., 1999; Peng et al., 2001; Chen et al., 2006; Gusmaroli et al., 2007; Hakenjos et al., 2011). β -Tubulin was detected with monoclonal antibodies (Sigma).

For densitometric analysis, mean intensities were background subtracted and normalized to the loading control using the ImageLab software v.5.1

Molecular Plant

(Bio-Rad), and each measurement represents the average from at least three independent experiments. Error bars in the graphs represent the SE of the mean ($n = 3$). Student's *t*-test was used for data validation (<http://graphpad.com/quickcalcs/ttest2.cfm>).

ACCESSION NUMBERS

Sequence data from this article are provided in Supplemental Table 2.

SUPPLEMENTAL INFORMATION

Supplemental Information is available at *Molecular Plant Online*.

FUNDING

This work was supported by a research grant from Ministero degli Esteri (Italy-Japan) PGR00145 to G.S., by research grants from Ministero dell'Istruzione, Università e Ricerca, Progetti di Ricerca di Interesse Nazionale, and from Sapienza Università di Roma to P.C., and funds from Franklin & Marshall College to P.D.J.

This article is also based upon work from COST Action (PROTEOSTASIS BM1307), supported by COST (European Cooperation in Science and Technology).

AUTHOR CONTRIBUTIONS

A.F., L.M., and P.D.J. planned and performed the experiments. K.D., N.H.M., A.B., and S.B. performed the experiments. P.V. and S.S. helped with experimental planning and revised the manuscript. P.C. participated in the experimental design, discussed the experiments, and revised the manuscript. P.D.J. and G.S. designed the research and wrote the article.

ACKNOWLEDGMENTS

We thank MinJun Feng for technical help, Haodong Chen and Xing-Wang Deng for providing the anti-CUL4 antibody and the *axr1-3* mutant, Claus Schwechheimer for providing the anti-NEDD8 antibody and Alessandra Franciosini for help with figure preparation. We also thank Ning Wei, Elah Pick, and Maria Lois for critical reading of the manuscript. No conflict of interest declared.

Received: March 10, 2015

Revised: July 29, 2015

Accepted: August 2, 2015

Published: August 12, 2015

REFERENCES

- Adachi, S., Uchimiya, H., and Umeda, M. (2006). Expression of B2-type cyclin-dependent kinase is controlled by protein degradation in *Arabidopsis thaliana*. *Plant Cell Physiol.* **47**:1683–1686.
- Barton, M.K., and Poethig, R.S. (1993). Formation of the shoot apical meristem in *Arabidopsis thaliana*: an analysis of development in the wild type and in the shoot meristemless mutant. *Development* **119**:823–831.
- Bennett, E.J., Rush, J., Gygi, S.P., and Harper, J.W. (2010). Dynamics of cullin-RING ubiquitin ligase network revealed by systematic quantitative proteomics. *Cell* **143**:951–965.
- Blilou, I., Xu, J., Wildwater, M., Willemsen, V., Paponov, I., Friml, J., Heidstra, R., Aida, M., Palme, K., and Scheres, B. (2005). The PIN auxin efflux facilitator network controls growth and patterning in *Arabidopsis* roots. *Nature* **433**:39–44.
- Cary, A.J., Che, P., and Howell, S.H. (2002). Developmental events and shoot apical meristem gene expression patterns during shoot development in *Arabidopsis thaliana*. *Plant J.* **32**:867–877.
- Chen, H., Shen, Y., Tang, X., Yu, L., Wang, J., Guo, L., Zhang, Y., Zhang, H., Feng, S., Strickland, E., et al. (2006). Arabidopsis CULLIN4 forms an E3 ubiquitin ligase with RBX1 and the CDD complex in mediating light control of development. *Plant Cell* **18**:1991–2004.
- Culligan, K.M., Robertson, C.E., Foreman, J., Doerner, P., and Britt, A.B. (2006). ATR and ATM play both distinct and additive roles in response to ionizing radiation. *Plant J.* **48**:947–961.
- Dekkers, B.J., Pearce, S., van Bolderen-Veldkamp, R.P., Marshall, A., Widera, P., Gilbert, J., Drost, H.-G.G., Bassel, G.W., Müller, K., King, J.R., et al. (2013). Transcriptional dynamics of two seed compartments with opposing roles in *Arabidopsis* seed germination. *Plant Physiol.* **163**:205–215.
- Dello Ioio, R., Linhares, F.S., Scacchi, E., Casamitjana-Martinez, E., Heidstra, R., Costantino, P., and Sabatini, S. (2007). Cytokinins determine *Arabidopsis* root-meristem size by controlling cell differentiation. *Curr. Biol.* **17**:678–682.
- Dharmasiri, N., Dharmasiri, S., Weijers, D., Lechner, E., Yamada, M., Hobbie, L., Ehrismann, J.S., Jurgens, G., and Estelle, M. (2005). Plant development is regulated by a family of auxin receptor F box proteins. *Dev. Cell* **9**:109–119.
- Dharmasiri, N., Dharmasiri, S., Weijers, D., Karunarathna, N., Jurgens, G., and Estelle, M. (2007). AXL and AXR1 have redundant functions in RUB conjugation and growth and development in *Arabidopsis*. *Plant J.* **52**:114–123.
- Dieterle, M., Thomann, A., Renou, J.P., Parmentier, Y., Cognat, V., Lemonnier, G., Muller, R., Shen, W.H., Kretsch, T., and Genschik, P. (2005). Molecular and functional characterization of *Arabidopsis* Cullin 3A. *Plant J.* **41**:386–399.
- Dohmann, E.M., Kuhnle, C., and Schwechheimer, C. (2005). Loss of the CONSTITUTIVE PHOTOMORPHOGENIC9 signalosome subunit 5 is sufficient to cause the *cop/det/fus* mutant phenotype in *Arabidopsis*. *Plant Cell* **17**:1967–1978.
- Dohmann, E.M., Levesque, M.P., De Veylder, L., Reichardt, I., Jurgens, G., Schmid, M., and Schwechheimer, C. (2008a). The *Arabidopsis* COP9 signalosome is essential for G2 phase progression and genomic stability. *Development* **135**:2013–2022.
- Dohmann, E.M., Levesque, M.P., Isono, E., Schmid, M., and Schwechheimer, C. (2008b). Auxin responses in mutants of the *Arabidopsis* CONSTITUTIVE PHOTOMORPHOGENIC9 signalosome. *Plant Physiol.* **147**:1369–1379.
- Dohmann, E.M., Nill, C., and Schwechheimer, C. (2010). DELLA proteins restrain germination and elongation growth in *Arabidopsis thaliana* COP9 signalosome mutants. *Eur. J. Cell. Biol.* **89**:163–168.
- Donnelly, P.M., Bonetta, D., Tsukaya, H., Dengler, R.E., and Dengler, N.G. (1999). Cell cycling and cell enlargement in developing leaves of *Arabidopsis*. *Dev. Biol.* **215**:407–419.
- Duda, D.M., Borg, L.A., Scott, D.C., Hunt, H.W., Hammel, M., and Schulman, B.A. (2008). Structural insights into NEDD8 activation of cullin-RING ligases: conformational control of conjugation. *Cell* **134**:995–1006.
- Enchev, R.I., Scott, D.C., da Fonseca, P.C., Schreiber, A., Monda, J.K., Schulman, B.A., Peter, M., and Morris, E.P. (2012). Structural basis for a reciprocal regulation between SCF and CSN. *Cell Rep.* **2**:616–627.
- Feng, S., Ma, L., Wang, X., Xie, D., Dinesh-Kumar, S.P., Wei, N., and Deng, X.W. (2003). The COP9 signalosome interacts physically with SCF COI1 and modulates jasmonate responses. *Plant Cell* **15**:1083–1094.
- Figuroa, P., Gusmaroli, G., Serino, G., Habashi, J., Ma, L., Shen, Y., Feng, S., Bostick, M., Callis, J., Hellmann, H., et al. (2005). *Arabidopsis* has two redundant Cullin3 proteins that are essential for embryo development and that interact with RBX1 and BTB proteins to form multisubunit E3 ubiquitin ligase complexes in vivo. *Plant Cell* **17**:1180–1195.
- Finkelstein, R., Reeves, W., Ariizumi, T., and Steber, C. (2008). Molecular aspects of seed dormancy. *Annu. Rev. Plant Biol.* **59**:387–415.

COP9 SIGNALOSOME in *Arabidopsis* Development

COP9 SIGNALLOSOME in *Arabidopsis* Development

Molecular Plant

- Fischer, E.S., Scrima, A., Bohm, K., Matsumoto, S., Lingaraju, G.M., Faty, M., Yasuda, T., Cavadini, S., Wakasugi, M., Hanaoka, F., et al. (2011). The molecular basis of CRL4DDB2/CSA ubiquitin ligase architecture, targeting, and activation. *Cell* **147**:1024–1039.
- Franciosini, A., Lombardi, B., Iafate, S., Pecce, V., Mele, G., Lupacchini, L., Rinaldi, G., Kondou, Y., Gusmaroli, G., Aki, S., et al. (2013). The *Arabidopsis* COP9 SIGNALLOSOME INTERACTING F-BOX KELCH 1 protein forms an SCF ubiquitin ligase and regulates hypocotyl elongation. *Mol. Plant* **6**:1616–1629.
- Friend, S.F., Peterson, L.K., Treacy, E., Stefanski, A.L., Sosinowski, T., Pennock, N.D., Berger, A.J., Winn, V.D., and Dragone, L.L. (2013). The discovery of a reciprocal relationship between tyrosine-kinase signaling and cullin neddylation. *PLoS One* **8**:e75200.
- Friml, J., Vieten, A., Sauer, M., Weijers, D., Schwarz, H., Hamann, T., Offringa, R., and Jurgens, G. (2003). Efflux-dependent auxin gradients establish the apical-basal axis of *Arabidopsis*. *Nature* **426**:147–153.
- Gabriele, S., Rizza, A., Martone, J., Circelli, P., Costantino, P., and Vittorioso, P. (2010). The Dof protein DAG1 mediates PIL5 activity on seed germination by negatively regulating GA biosynthetic gene AtGA3ox1. *Plant J.* **61**:312–323.
- Gordon, S.P., Heisler, M.G., Reddy, G.V., Ohno, C., Das, P., and Meyerowitz, E.M. (2007). Pattern formation during de novo assembly of the *Arabidopsis* shoot meristem. *Development* **134**:3539–3548.
- Gray, W.M., del Pozo, J.C., Walker, L., Hobbie, L., Risseuw, E., Banks, T., Crosby, W.L., Yang, M., Ma, H., and Estelle, M. (1999). Identification of an SCF ubiquitin-ligase complex required for auxin response in *Arabidopsis thaliana*. *Genes Dev.* **13**:1678–1691.
- Gusmaroli, G., Feng, S., and Deng, X.W. (2004). The *Arabidopsis* CSN5A and CSN5B subunits are present in distinct COP9 signalosome complexes, and mutations in their JAMM domains exhibit differential dominant negative effects on development. *Plant Cell* **16**:2984–3001.
- Gusmaroli, G., Figueroa, P., Serino, G., and Deng, X.W. (2007). Role of the MPN subunits in COP9 signalosome assembly and activity, and their regulatory interaction with *Arabidopsis* Cullin3-based E3 ligases. *Plant Cell* **19**:564–581.
- Hakenjos, J.P., Richter, R., Dohmann, E.M., Katsiarimpa, A., Isono, E., and Schwechheimer, C. (2011). MLN4924 is an efficient inhibitor of NEDD8 conjugation in plants. *Plant Physiol.* **156**:527–536.
- Heidstra, R., and Sabatini, S. (2014). Plant and animal stem cells: similar yet different. *Nat. Rev. Mol. Cell Biol.* **15**:301–312.
- Hind, S.R., Pulliam, S.E., Veronese, P., Shantharaj, D., Nazir, A., Jacobs, N.S., and Stratmann, J.W. (2011). The COP9 signalosome controls jasmonic acid synthesis and plant responses to herbivory and pathogens. *Plant J.* **65**:480–491.
- Hotton, S.K., and Callis, J. (2008). Regulation of cullin RING ligases. *Annu. Rev. Plant Biol.* **59**:467–489.
- Irigoyen, M.L., Iniesto, E., Rodriguez, L., Puga, M.I., Yanagawa, Y., Pick, E., Strickland, E., Paz-Ares, J., Wei, N., De Jaeger, G., et al. (2014). Targeted degradation of abscisic acid receptors is mediated by the ubiquitin ligase substrate adaptor DDA1 in *Arabidopsis*. *Plant Cell* **26**:712–728.
- Jenik, P.D., Jurkuta, R.E., and Barton, M.K. (2005). Interactions between the cell cycle and embryonic patterning in *Arabidopsis* uncovered by a mutation in DNA polymerase epsilon. *Plant Cell* **17**:3362–3377.
- Jurkuta, R.J., Kaplinsky, N.J., Spindel, J.E., and Barton, M.K. (2009). Partitioning the apical domain of the *Arabidopsis* embryo requires the BOBBER1 NudC domain protein. *Plant Cell* **21**:1957–1971.
- Kawakami, T., Chiba, T., Suzuki, T., Iwai, K., Yamanaka, K., Minato, N., Suzuki, H., Shimbara, N., Hidaka, Y., Osaka, F., et al. (2001). NEDD8 recruits E2-ubiquitin to SCF E3 ligase. *EMBO J.* **20**:4003–4012.
- Kwok, S.F., Piekos, B., Misera, S., and Deng, X.W. (1996). A complement of ten essential and pleiotropic *Arabidopsis* COP/DET/FUS genes is necessary for repression of photomorphogenesis in darkness. *Plant Physiol.* **110**:731–742.
- Kwok, S.F., Solano, R., Tsuge, T., Chamovitz, D.A., Ecker, J.R., Matsui, M., and Deng, X.W. (1998). *Arabidopsis* homologs of a c-Jun coactivator are present both in monomeric form and in the COP9 complex, and their abundance is differentially affected by the pleiotropic *cop/det/fus* mutations. *Plant Cell* **10**:1779–1790.
- Kwok, S.F., Staub, J.M., and Deng, X.W. (1999). Characterization of two subunits of *Arabidopsis* 19S proteasome regulatory complex and its possible interaction with the COP9 complex. *J. Mol. Biol.* **285**:85–95.
- Le, B.H., Cheng, C., Bui, A.Q., Wagmaister, J.A., Henry, K.F., Pelletier, J., Kwong, L., Belmonte, M., Kirkbride, R., Horvath, S., et al. (2010). Global analysis of gene activity during *Arabidopsis* seed development and identification of seed-specific transcription factors. *Proc. Natl. Acad. Sci. USA* **107**:8063–8070.
- Lingaraju, G.M., Bunker, R.D., Cavadini, S., Hess, D., Hassiepen, U., Renatus, M., Fischer, E.S., and Thoma, N.H. (2014). Crystal structure of the human COP9 signalosome. *Nature* **512**:161–165.
- Lyapina, S., Cope, G., Shevchenko, A., Serino, G., Tsuge, T., Zhou, C., Wolf, D.A., Wei, N., Shevchenko, A., and Deshaies, R.J. (2001). Promotion of NEDD-CUL1 conjugate cleavage by COP9 signalosome. *Science* **292**:1382–1385.
- Lydeard, J.R., Schulman, B.A., and Harper, J.W. (2013). Building and remodelling Cullin-RING E3 ubiquitin ligases. *EMBO Rep.* **14**:1050–1061.
- McNellis, T.W., von Arnim, A.G., Araki, T., Komeda, Y., Misera, S., and Deng, X.W. (1994). Genetic and molecular analysis of an allelic series of *cop1* mutants suggests functional roles for the multiple protein domains. *Plant Cell* **6**:487–500.
- Misera, S., Muller, A.J., Weiland-Heidecker, U., and Jurgens, G. (1994). The FUSCA genes of *Arabidopsis*: negative regulators of light responses. *Mol. Gen. Genet.* **244**:242–252.
- Möller, B., and Weijers, D. (2009). Auxin control of embryo patterning. *Gold Spring Harb. Perspect. Biol.* **1**:a001545.
- Pan, L., Wang, S., Lu, T., Weng, C., Song, X., Park, J.K., Sun, J., Yang, Z.H., Yu, J., Tang, H., et al. (2014). Protein competition switches the function of COP9 from self-renewal to differentiation. *Nature* **514**:233–236.
- Peng, Z., Staub, J.M., Serino, G., Kwok, S.F., Kurepa, J., Bruce, B.D., Vierstra, R.D., Wei, N., and Deng, X.W. (2001). The cellular level of PR500, a protein complex related to the 19S regulatory particle of the proteasome, is regulated in response to stresses in plants. *Mol. Biol. Cell* **12**:383–392.
- Petroski, M.D., and Deshaies, R.J. (2005). Function and regulation of cullin-RING ubiquitin ligases. *Nat. Rev. Mol. Cell Biol.* **6**:9–20.
- Qian, Y., Ng, C.L., and Schulz, C. (2015). CSN maintains the germline cellular microenvironment and controls the level of stem cell genes via distinct CRLs in testes of *Drosophila melanogaster*. *Dev. Biol.* **398**:68–79.
- Rao, F., Xu, J., Khan, A.B., Gadalla, M.M., Cha, J.Y., Xu, R., Tyagi, R., Dang, Y., Chakraborty, A., and Snyder, S.H. (2014). Inositol hexakisphosphate kinase-1 mediates assembly/disassembly of the CRL4-signalosome complex to regulate DNA repair and cell death. *Proc. Natl. Acad. Sci. USA* **111**:16005–16010.
- Raz, V., Bergervoet, J.H., and Koornneef, M. (2001). Sequential steps for developmental arrest in *Arabidopsis* seeds. *Development* **128**:243–252.
- Sabatini, S., Beis, D., Wolkenfelt, H., Murfett, J., Guilfoyle, T., Malamy, J., Benfey, P., Leyser, O., Bechtold, N., Weisbeek, P., et al. (1999).

Molecular Plant

An auxin-dependent distal organizer of pattern and polarity in the *Arabidopsis* root. *Cell* **99**:463–472.

- Sabatini, S., Heidstra, R., Wildwater, M., and Scheres, B.** (2003). SCARECROW is involved in positioning the stem cell niche in the *Arabidopsis* root meristem. *Genes Dev.* **17**:354–358.
- Sassi, M., Lu, Y., Zhang, Y., Wang, J., Dhonukshe, P., Bilou, I., Dai, M., Li, J., Gong, X., Jaillais, Y., et al.** (2012). COP1 mediates the coordination of root and shoot growth by light through modulation of PIN1- and PIN2-dependent auxin transport in *Arabidopsis*. *Development* **139**:3402–3412.
- Schmidt, M.W., McQuary, P.R., Wee, S., Hofmann, K., and Wolf, D.A.** (2009). F-box-directed CRL complex assembly and regulation by the CSN and CAND1. *Mol. Cell* **35**:586–597.
- Schwechheimer, C., Serino, G., Callis, J., Crosby, W.L., Lyapina, S., Deshaies, R.J., Gray, W.M., Estelle, M., and Deng, X.W.** (2001). Interactions of the COP9 signalosome with the E3 ubiquitin ligase SCFTIR1 in mediating auxin response. *Science* **292**:1379–1382.
- Serino, G., Su, H., Peng, Z., Tsuge, T., Wei, N., Gu, H., and Deng, X.W.** (2003). Characterization of the last subunit of the *Arabidopsis* COP9 signalosome: implications for the overall structure and origin of the complex. *Plant Cell* **15**:719–731.
- Shabek, N., and Zheng, N.** (2014). Plant ubiquitin ligases as signaling hubs. *Nat. Struct. Mol. Biol.* **21**:293–296.
- Stuttman, J., Lechner, E., Guerois, R., Parker, J.E., Nussaume, L., Genschik, P., and Noel, L.D.** (2009). COP9 signalosome- and 26S proteasome-dependent regulation of SCFTIR1 accumulation in *Arabidopsis*. *J. Biol. Chem.* **284**:7920–7930.
- Wang, X., Feng, S., Nakayama, N., Crosby, W.L., Irish, V., Deng, X.W., and Wei, N.** (2003). The COP9 signalosome interacts with SCF UFO and participates in *Arabidopsis* flower development. *Plant Cell* **15**:1071–1082.
- Wee, S., Geyer, R.K., Toda, T., and Wolf, D.A.** (2005). CSN facilitates Cullin-RING ubiquitin ligase function by counteracting autocatalytic adapter instability. *Nat. Cell Biol.* **7**:387–391.
- Wei, N., and Deng, X.W.** (1992). COP9: a new genetic locus involved in light-regulated development and gene expression in *Arabidopsis*. *Plant Cell* **4**:1507–1518.
- Wei, N., Kwok, S.F., von Arnim, A.G., Lee, A., McNellis, T.W., Piekos, B., and Deng, X.W.** (1994). *Arabidopsis* COP8, COP10, and COP11 genes are involved in repression of photomorphogenic development in darkness. *Plant Cell* **6**:629–643.
- Wei, N., Serino, G., and Deng, X.W.** (2008). The COP9 signalosome: more than a protease. *Trends Biochem. Sci.* **33**:592–600.
- Willmann, M.R., Mehalick, A.J., Packer, R.L., and Jenik, P.D.** (2011). MicroRNAs regulate the timing of embryo maturation in *Arabidopsis*. *Plant Physiol.* **155**:1871–1884.
- Winter, D., Vinegar, B., Nahal, H., Ammar, R., Wilson, G.V., and Provart, N.J.** (2007). An “Electronic Fluorescent Pictograph” browser for exploring and analyzing large-scale biological data sets. *PLoS One* **2**:e718.
- Wysocka-Diller, J.W., Helariutta, Y., Fukaki, H., Malamy, J.E., and Benfey, P.N.** (2000). Molecular analysis of SCARECROW function reveals a radial patterning mechanism common to root and shoot. *Development* **127**:595–603.
- Zemla, A., Thomas, Y., Kedziora, S., Knebel, A., Wood, N.T., Rabut, G., and Kurz, T.** (2013). CSN- and CAND1-dependent remodelling of the budding yeast SCF complex. *Nat. Commun.* **4**:1641.